This is a preprint, the final version is subject to change, of the American Mineralogist (MSA)
Cite as Authors (Year) Title. American Mineralogist, in press.
(DOI will not work until issue is live.) DOI: http://dx.doi.org/10.2138/am-2016-5844

Revision 1

Wayneburnhamite, $Pb_9Ca_6(Si_2O_7)_3(SiO_4)_3$, an apatite polysome – the Mn-free analogue of ganomalite from Crestmore, California.

ANTHONY R. KAMPF[1]*, ROBERT M. HOUSLEY[2], AND GEORGE R. ROSSMAN[2]

[1]Mineral Sciences Department, Natural History Museum of Los Angeles County, 900 Exposition Boulevard, Los Angeles, CA 90007, USA

[2]Division of Geological and Planetary Sciences, California Institute of Technology, Pasadena, CA 91125, USA

*Email: akampf@nhm.org

Abstract

Wayneburnhamite (IMA2015-124), $Pb_9Ca_6(Si_2O_7)_3(SiO_4)_3$, is a new mineral from the Commercial quarry, Crestmore, Riverside County, California, where it occurs as a metasomatic mineral on fracture surfaces in vesuvianite/wollastonite rock. Wayneburnhamite crystals are sky-blue hexagonal tablets and prisms up to 0.5 mm in maximum dimension. The streak is white. Crystals are transparent to translucent with vitreous to resinous luster. The Mohs hardness is 3½, the tenacity is brittle, the fracture is conchoidal, and there is no cleavage. The calculated density is 5.271 g/cm^3. The mineral is optically uniaxial (+), with $\omega = 1.855(5)$ and $\varepsilon = 1.875(5)$ (white light). The pleochroism is *E* sky blue and *O* lighter sky blue; $E > O$ weak. Raman and infrared spectra are consistent with the crystal structure, but suggest a very minor hydrous component.

The empirical formula (based on 9 Si *apfu*) is $(Pb_{8.33}Sr_{0.04}\square_{0.63})_{\Sigma 9.00}(Ca_{5.40}Cu^{2+}_{0.27}\square_{0.33})_{\Sigma 6.00}Si_9S_{0.21}O_{32.64}Cl_{0.05}$. Wayneburnhamite is hexagonal, *P*-6, a = 9.8953(9), c = 10.2054(7) Å, V = 865.40(17) Å^3, and Z = 1. The eight strongest lines in the X-ray powder diffraction pattern are [d_{obs} in Å(*I*)(*hkl*)]: 4.95(52)(110); 4.45(64)(111); 3.550(77)(112); 3.232(54)(120); 3.086(100)(121); 2.847(60)(300); 2.798(48)(113); and 2.734(83)(212). The structure determination (R_1 = 3.01% for 1063 $F_o > 4\sigma F$) shows wayneburnhamite to be an apatite polysome isostructural with ganomalite, differing only in that the site occupied dominantly by Mn in the structure of ganomalite is occupied dominantly by Ca in the structure of wayneburnhamite. The structure refinement of wayneburnhamite appears to represent a rare case in which the approximate locations of the Pb^{2+} $6s^2$ lone-electron pairs can be seen as electron density residuals.

Keywords: wayneburnhamite; new mineral; crystal structure; spectroscopy; apatite polysome; ganomalite; lone-electron pairs; Crestmore, California.

Introduction

Ganomalite was first described from Långban, Sweden by Nordenskiöld (1876, 1877). In 1899, Penfield and Warren conjectured that ganomalite was the hydroxyl analogue of nasonite, $Pb_9Ca_4Si_6O_{21}Cl_2$ and this relation was generally accepted until 1972, when Engel showed that, based upon its similarity in symmetry and cell parameters to several synthetic phases, ganomalite probably had a structure intermediate between those of nasonite and apatite. Dunn et al. (1985) noted that chemical analyses of material from Långban and Jacobsberg, Sweden, and from Franklin, New Jersey, U.S.A., all exhibited significant contents of Mn. Furthermore, the

preliminary crystal structure data of Dunn et al. (1985) showed that Mn and Ca are ordered in the structure and that Mn is dominant in one site, making it an essential element in ganomalite, which has the ideal formula $Pb_9Ca_5MnSi_9O_{33}$. This formula can be recast as $Pb_9Ca_5Mn(Si_2O_7)_3(SiO_4)_3$ to indicate the presence in the structure of both sorosilicate and nesosilicate groups. In 1997, Carlson and Norrestam provided a full crystal structure determination for ganomalite from Jacobsberg, Sweden, which confirmed the findings of Dunn et al. (1985). More recently, Baikie et al. (2010) presented a formal description of apatite polysomes with the general formula $A_{5N}B_{3N}O_{9N+6}X_{N\delta}$ ($2 \leq N \leq \infty$), where A designates the large cations in the framework (A^F) and in the tunnels (A^T), B designates the cation in the tetrahedral site, and X designates the anion (if any) in the tunnel; $N = 2$ for pyromorphite $[Pb_{10}(PO_4)_6Cl_2]$, $N = 3$ for ganomalite $[Pb_9Ca_6(Si_2O_7)_3(SiO_4)_3\square_3]$, and $N = 4$ for nasonite $[Pb_{12}Ca_8(Si_2O_7)_6Cl_4]$.

Ganomalite was reported as "gray coatings and druses" from the Commercial quarry at Crestmore, California, by DeVito et al. (1971) based upon a personal communication from Joseph Murdoch, but no chemical analysis was reported. Fred DeVito had collected excellent hexagonal prismatic blue crystals at Crestmore in 1964, which were only later identified as ganomalite. We examined two of the specimens collected in 1964 by DeVito and found the crystals to correspond to ganomalite in all respects, except that they contain, at most, a trace of Mn. The Crestmore crystals, therefore, correspond to a new species, distinct from ganomalite and with the ideal formula $Pb_9Ca_6(Si_2O_7)_3(SiO_4)_3$.

The new mineral is named wayneburnhamite in honor of American geochemist-petrologist Dr. C. Wayne Burnham (1922–2015). Dr. Burnham had a long and illustrious career as Professor at Pennsylvania State University from 1955–1986 and then as Adjunct Professor of Geology at Arizona State University for many years. He is best known for his seminal research

on the role of volatiles in igneous systems, which in a real sense had a revolutionary impact on modern igneous petrology. It is largely for his work in this area that he was awarded the 1998 Roebling Medal by the Mineralogical Society of America. Burnham's interest in minerals and geology was awakened when, after serving in World War II, he joined his older brother George in establishing what was to become a well-known mineral business, Burminco. This led him to decide to pursue a degree in geology at Pomona College where he wrote a thesis on the "Geology of the Crestmore Quarries", which was published in *California Division of Mines Bulletin* **170** as "Contact metamorphism at Crestmore, California". Subsequently, this was also the basis for Burnham's 1959 publication "Contact metamorphism of magnesian limestones at Crestmore" (see references). Burnham graduated from Pomona College in 1951 and received his Ph.D. in geochemistry from Caltech in 1955.

The new mineral and name have been approved by the Commission on New Minerals, Nomenclature, and Classification of the International Mineralogical Association (IMA2015-124). The description is based on one holotype and one cotype specimen housed in the collections of the Mineral Sciences Department, Natural History Museum of Los Angeles County, 900 Exposition Boulevard, Los Angeles, California 90007, USA, catalogue numbers 65639 (holotype) and 65640 (cotype).

Occurrence and paragenesis

Wayneburnhamite was found in the Commercial quarry, Crestmore, Sky Blue Hill, Riverside County, California, USA (34°01'24.6"N 117°23'04.6"W). The specimens examined were collected by the late Fred DeVito in 1964. The cotype is a very small (~2 mm diameter) fragment used for SEM/EDS study that was provided by Fred DeVito. The holotype is a 4 × 4 ×

1.5 cm matrix specimen that was provided by Thomas Loomis from the Fred DeVito Collection. Previous reports (e.g. DeVito et al. 1971) identified this mineral as ganomalite and we are convinced that all other specimens of "ganomalite" from Crestmore are actually wayneburnhamite.

The world famous Crestmore deposit was mined for calcite used in the manufacture of cement. Operations at several quarries and extensive underground workings exploiting the deposit began in 1909 and ceased in 1986. The deposit formed as the result of the intrusion of a quartz monzonite porphyry into a magnesian limestone. The intrusion formed an extensive contact metamorphic aureole consisting of several zones and the release of water and other volatiles resulted in large-scale metasomatism. The most detailed study of the deposit was by Burnham (1959), DeVito et al. (1971) provided the most complete account of Crestmore minerals, and the report of a discovery of remarkable clintonite crystals by Forrester (2003) is the most recent publication on the deposit.

On the holotype specimen, wayneburnhamite occurs with whelanite on fracture surfaces in vesuvianite/wollastonite rock with accessory grossular. On the cotype specimen, it occurs on calcite in association with cerussite, whelanite and a currently uncharacterized Ca-Pb-Sb-silicate. DeVito et al. (1971) also note nasonite as an associated mineral. Wayneburnhamite is presumed to have formed during metasomatism with galena in the limestone serving as the source of the Pb.

Physical and optical properties

Wayneburnhamite crystals are hexagonal tablets and prisms up to 0.5 mm in maximum dimension, as individuals and intergrowths (Figs. 1 and 2). The forms exhibited are {100} and

{001}, occasionally modified by {101} and/or {011} (Fig. 3). These crystals are sky blue and transparent on margins, varying to nearly colorless and cloudy in interiors (note that the blue color is attributed to Cu^{2+}, which is not essential to the formula). The mineral is also found as purple-gray drusy coatings of indistinct crystals. The mineral has white streak and vitreous to resinous luster. Wayneburnhamite does not fluoresce in long- or short-wave ultraviolet light. The Mohs hardness is 3½, the tenacity is brittle, the fracture is conchoidal, and there is no cleavage. The density could not be measured because it is greater than available density liquids and there is insufficient material for physical measurement. The calculated density is 5.271 g/cm^3 using the empirical formula and 5.537 g/cm^3 using the ideal formula. Wayneburnhamite decomposes readily in room temperature dilute HCl and HNO_3, decomposes very slowly in dilute or concentrated H_2SO_4, and is unreactive in a saturated solution of NaOH.

The mineral is uniaxial (+), with $\omega = 1.855(5)$ and $\varepsilon = 1.875(5)$ (determined in white light). The pleochroism is *E* sky blue and *O* lighter sky blue; $E > O$ weak. The Gladstone-Dale compatibility, $1 - (K_p/K_c)$ is –0.034 (excellent) for the empirical formula and 0.011 (superior) for the ideal formula (Mandarino 2007).

Spectroscopy

Raman

Raman spectroscopic microanalyses were carried out on the microprobe polished sample of wayneburnhamite, as well as on a crystal of ganomalite from the Jacobsberg mine, Varmland, Sweden in the collection of the Natural History Museum of Los Angeles County, catalogue number 45523. The identity of the ganomalite crystal was confirmed by powder X-ray diffraction. Spectra were recorded using a Renishaw M1000 micro-Raman spectrometer system.

Light from a 514.5 nm solid-state laser was focused onto the samples with a 100× objective lens. Approximately 6 mW of laser power was available at the samples in a spot size of about 1 μm diameter, but to avoid any possible sample damage only 10% power was used. Peak positions were calibrated against a silicon (520.5 cm^{-1}) standard. All spectra were obtained with a dual-wedge polarization scrambler inserted directly above the objective lens to minimize the effects of polarization. The wayneburnhamite Raman spectrum (Fig. 4) exhibits prominent features at shifts of 3587, 1043, 851, 564, 549, and 371 cm^{-1}. The 3587 band is in the OH stretching region suggesting that a hydrous species (H_2O or OH) is in wayneburnhamite. The 1043 band and the 564, 549 pair are in the typical tetrahedral silicate vibration regions. The spectrum of ganomalite (Fig. 4) closely resembles that of wayneburnhamite, although it lacks the band around 3600 cm^{-1}. Ganomalite's prominent features are at 1042, 848, 564, 551, and 373 cm^{-1}. It is noteworthy that the ganomalite spectrum on the RRUFF database (Lafuente et al. 2015) is quite different, suggesting that this spectrum was obtained on a different phase.

Infrared

To address the possibility that there is a hydroxide or water component in the mineral, transmission spectra were obtained through both the sample used for the electron microprobe analysis that was epoxied to a microscope slide, and through a separate, free-standing crystal oriented as a (0001) plate (Fig. 5). The measurements were made with a Nicolet Continμum FTIR microscope attached to a Thermo-Nicolet iS50 FTIR. The spectrum of the electron microprobe mount was obtained with linearly polarized light in the two extinctions directions, only one of which was a principal direction of the indicatrix. The spectra of both samples show a prominent, broad, asymmetrical absorption feature in the water region with a maximum at about

3383 cm^{-1}, a low-intensity absorption band centred at 5148 cm^{-1} where combined stretching and bending of water molecules occurs, and a less-intense, sharper feature at 3579 cm^{-1}, consistent with an OH stretching absorption band.

The 0.035 mm thick crystal in the electron microprobe mount was oriented in an intermediate orientation such that the **c**-axis was neither in the plane of the slide or perpendicular to it. This allowed spectra to be obtained polarized in the two extinction directions, one perpendicular to **c** and the other in a position intermediate between parallel and perpendicular to **c**. These spectra showed that the sharper OH feature near 3583 cm^{-1} has 2/3 the intensity in the intermediate position compared to the **E** parallel to **c** position. This suggests that the OH group is structurally incorporated in wayneburnhamite. There is little difference in the intensity of the broader feature in the two polarizations.

To estimate the content of water giving rise to the broad absorption feature centred near 3375 cm^{-1} we performed a Beer's law calculation. For the absorption intensity (molar absorptivity, ε) of liquid water, we used 223 $l \cdot mol^{-1} \cdot cm^{-1}$, the average of the values of 220 $l \cdot mol^{-1} \cdot cm^{-1}$ from Wieliczka et al. (1989), and 227 $l \cdot mol^{-1} \cdot cm^{-1}$ from Hale and Querry (1973). From the intensity of the absorption band in the spectrum of the 273 μm thick crystal, the calculation leads to a water content of 0.11% by weight, assuming a density of 5.271 $g \cdot cm^{-3}$ for wayneburnhamite. The water content seems too low to be a stoichiometric component, but too high to ignore as minor contamination. Most likely, the water is contained in the pervasive porosity of the samples that is a cause of the turbidity in their interiors.

The amount of OH represented by the sharp absorption near 3579 cm^{-1} was estimated with a Beer's law calculation using a representative ε value of 100 $l \cdot mol^{-1} \cdot cm^{-1}$ using the **E** perpendicular to **c** spectra of both the microprobe mount and the free-standing crystal. Both

185 calculations gave an OH content, expressed as wt% H_2O, of 0.021%, a value typical for minor
186 OH traces commonly found in many anhydrous minerals, but unrelated to the ideal
187 stoichiometry.
188
189 **Chemical composition**
190 Chemical analyses (6 points on 3 crystals) were carried out using a JEOL 8200 electron
191 microprobe (WDS mode, 15 kV, 20 nA and focused beam) at the Division of Geological and
192 Planetary Sciences, California Institute of Technology. No other elements were detected in EDS
193 analyses. There was no apparent beam damage; however, ubiquitous crystal porosity resulted in
194 low analytical totals. Minor oscillatory compositional zonation was noted with higher Pb/Ca in
195 the cores and on the rims and lower Pb/Ca in the intermediate regions. The results are given in
196 Table 1. The empirical formula (based on 9 Si *apfu*) is
197 $(Pb_{8.33}Sr_{0.04}\square_{0.63})_{\Sigma 9.00}(Ca_{5.40}Cu^{2+}_{0.27}\square_{0.33})_{\Sigma 6.00}Si_9S_{0.21}O_{32.64}Cl_{0.05}$. The simplified formula is
198 $Pb_9Ca_6(Si_2O_7)_4(SiO_4)O$, which requires PbO 69.60, CaO 11.66, SiO_2 18.74, total 100 wt%.
199
200 **X-ray crystallography and structure refinement**
201 Both powder and single-crystal X-ray studies were carried out using a Rigaku R-Axis
202 Rapid II curved imaging plate microdiffractometer, with monochromatized Mo$K\alpha$ radiation. For
203 the powder-diffraction study, a Gandolfi-like motion on the φ and ω axes was used to randomize
204 the sample and observed *d*-values and intensities were derived by profile fitting using JADE 2010
205 software (Materials Data, Inc.). The powder data are presented in Table 2 (deposited). Unit-cell
206 parameters refined from the powder data using JADE 2010 with whole pattern fitting are a =
207 9.850(4), c = 10.162(4) Å and V = 853.9(8) Å^3.

The Rigaku CrystalClear software package was used for processing structure data, including the application of an empirical multi-scan absorption correction using ABSCOR (Higashi 2001). The structure was solved by direct methods using SIR2011 (Burla et al. 2012) and then the coordinates were transformed to correspond to those reported by Carlson and Norrestam (1997) for the structure of ganomalite. SHELXL-2013 (Sheldrick 2008) was used for the refinement of the structure. The two Pb sites, Pb1 and Pb2, refined to occupancies of 0.926 and 0.928, respectively. The Ca2 and Ca3 sites refined to full occupancy by Ca. The Ca1 and Ca4 sites displayed higher scattering powers and shorter <Ca–O>; consequently, they were refined with joint occupancy by Ca and Cu, yielding $Ca_{0.80}Cu_{0.20}$ and $Ca_{0.71}Cu_{0.29}$, for the Ca1 and Ca4 sites, respectively. The Si and O sites were assigned full occupancies. The resulting structural formula, $(Pb_{8.34}\square_{0.66})_{\Sigma 9.00}(Ca_{5.31}Cu^{2+}_{0.69})_{\Sigma 6.00}(Si_2O_7)_3(SiO_4)_3$, is a fair fit to the empirical formula, although the amount of Cu indicated by the structure refinement is consistent with a Cu content toward the upper end of the range of EPMA analyses. With all atoms assigned anisotropic displacement parameters, the refinement yielded $R_1 = 0.0301$ for 1063 $F_o > 4\sigma F$ reflections. Two of the four highest electron density residuals, 2.46 and 1.81 e/A^3, are located within the tunnels at [0.192, 0.187, 0.203] and [0.026, 0.203, ½], 0.80 and 0.79 Å from Pb1 and Pb2, respectively. Modelling these residuals as He atoms as a proxy for lone-pair electrons, assigning them isotropic displacement parameters of 0.02 Å^2, and holding their positions invariant reduced R_1 to 0.0275; nevertheless, we report herein the results of the refinement without the residuals modelled as He atoms. Details of the data collection and structure refinement are provided in Table 3. Fractional coordinates and atom displacement parameters are provided in Table 4, and selected interatomic distances in Table 5. Reasonable bond-valence sums were found for all sites, as seen in Table 6 (deposited).

Discussion

The structure of wayneburnhamite (Figs. 6 and 7) is essentially the same as that of ganomalite (Dunn et al. 1985; Carlson and Norrestam 1997), differing only in that the site occupied dominantly by Mn in the structure of ganomalite is occupied dominantly by Ca in the structure of wayneburnhamite. The structure contains face-sharing chains of CaO_6 polyhedra parallel to [001]. The Ca2 and Ca4 coordinations are trigonal prisms, whereas the Ca1 and Ca3 coordinations are twisted trigonal prisms (metaprisms). The Ca2 and Ca3 sites each have three additional longer Ca–O bonds providing 9(6+3)-coordinations that can be described as square anti-prisms, which are not shown in Figures 6 and 7. The face-sharing chains of Ca–O polyhedra are linked by both SiO_4 and Si_2O_7 groups, yielding a framework with large channels along [001]. The two Pb sites, with lopsided 7-coordinations, are arranged around the periphery of the channel forming what Carlson and Norrestam (1997) referred to as a 'lead tunnel'. No other atom sites are located within the tunnel.

The lopsided coordinations of Pb1 and Pb2 are indicative of stereoactive Pb^{2+} $6s^2$ lone-electron pairs. Carlson and Norrestam (1997) assumed that the lone-pairs point into the tunnel; however, they provided no indication that they observed residual electron density in the tunnel that could be interpreted as direct evidence of the lone-pairs. In our refinement, two of the four highest electron density residuals, 2.46 and 1.81 e/A^3, are located within the tunnels at [0.192, 0.187, 0.203] and [0.026, 0.203, ½], 0.80 and 0.79 Å from Pb1 and Pb2, respectively (Fig. 6). This appears to represent a rare case in which the approximate locations of the Pb^{2+} $6s^2$ lone-electron pairs can be seen as distinct electron density residuals.

253 The Ca4 site in the structure of wayneburnhamite corresponds to the Mn site in the
254 ganomalite structure. The Ca4 site, while the smallest of the Ca sites in wayneburnhamite (<Ca4–
255 O> = 2.35 Å), is much larger than the Mn site in the structure of ganomalite. Dunn et al. (1985)
256 reported an average Mn–O distance of 2.18 Å and Carlson and Norrestam (1997) reported an
257 average Mn–O distance of 2.249 Å, the latter being for a site containing 56% Mn and 44% Ca.
258 Baikie et al. (2010) provide a detailed discussion of the polysomatic relationship between
259 the structures of apatite, ganomalite, and nasonite. Rather than repeat their diagrams here, we
260 refer the reader to their paper. The structural frameworks of the apatite polysomes appear
261 essentially identical when viewed along **c**, the direction of the 'lead tunnel' (cf. Fig. 6); however,
262 viewed perpendicular to **c** (cf. Fig. 7), the polysomatic relationship becomes clear. The structure
263 of wayneburnhamite/ganomalite is seen in Figure 7 to possess alternating SiO_4 and Si_2O_7 along
264 the **c**. By contrast, the apatite structure contains only isolated PO_4 groups and the nasonite
265 structure contains only Si_2O_7 groups.
266 As demonstrated by Baikie et al. (2010) for apatite polysomes, the stacking of modules
267 determines the linkages between the tetrahedra and these, in turn, determine whether the
268 coordination polyhedra of the large framework cations are regular trigonal prisms or twisted
269 prisms (metaprisms). In the apatite structure, all tetrahedra are isolated and all large framework
270 polyhedra are metaprisms, although the degree of metaprism twist (twist angle) varies depending
271 on the composition (White et al. 2005). For both the wayneburnhamite/ganomalite and nasonite
272 structures, those large framework polyhedra that have edges bridged by Si_2O_7 groups are regular
273 trigonal prisms, while those that do not have edges bridged by Si_2O_7 groups are metaprisms. As
274 noted above and easily seen in Figure 7, the Ca2 and Ca4 trigonal prisms in the structure of

wayneburnhamite both have edges bridged by Si_2O_7 groups, and the Ca1 and Ca3 metaprisms do not.

In reference to the dominance of Mn at one of the large framework-cation sites, Dunn et al. (1985) stated that "There is therefore a strong implication that Mn (or a cation of similar radius; perhaps Fe^{2+} or Mg) is essential to the stability of ganomalite." Our determination of the structure of wayneburnhamite clearly shows that not to be the case; however, the question remaining to be answered is why Mn^{2+} so strongly prefers one of the four large framework-cation sites over the others. Neither Dunn et al. (1985) nor Carlson and Norrestam (1997) consider this question. Baikie et al. (2010) note that, in the ganomalite structure, the sites with metaprism coordinations (Ca1 and Ca3) are fully occupied by the larger Ca^{2+}, while the Mn^{2+}-dominant site has a trigonal prism coordination; however, they do not mention the fact that the Ca2 site also has a trigonal prism coordination polyhedron, yet is fully occupied by Ca^{2+} with <Ca–O> = 2.41 Å.

In spite of the similar coordination geometries of the Ca2 and Ca4 (= Mn) sites in the wayneburnhamite (ganomalite) structure, the sites differ in that the Ca2 site is coordinated to three additional O atoms at greater distance, but the Ca4 site is not. This difference seems to explain the preference of the smaller Mn^{2+} for the Ca4 site and, in turn, the presence of Mn in that site drives a further reduction in the bond lengths.

Implications

The apatite structure is particularly noteworthy for its ability to accommodate a broad range of cations and anions (cf. Pan and Fleet 2002; Hughes and Rakovan 2015) and for its directional microporous properties related to its tunnels (cf. White et al. 2005). In contrast to materials with the apatite structure, synthetic apatite polysomes have been far less studied. The

phase $Pb_{15}(Ge_2O_7)_3(GeO_4)_3$, isostructural with ganomalite, has received considerable attention dating back to the 1970s because of its ferro- and pyroelectric functionality and its reversible optical activity. A variety of other ganomalite-structure synthetics have also been studied, as have a much smaller number of nasonite-structure phases (see Baikie et al. 2010 and references therein). It appears that, beyond the studies of the ganomalite structure by Dunn et al. (1985) and Carlson and Norrestam (1997), no attention has been paid to the possible ordering of different sized cations in the large framework-cation sites in ganomalite-type structures. The natural occurrence of wayneburnhamite clearly demonstrates the stability of the ganomalite structure with the formula $Pb_9Ca_6(Si_2O_7)_3(SiO_4)_3$, that is, without the presence of Mn^{2+} or a similar small-size cation in the Ca4 site. At the same time, it highlights the possibility that cations of different sizes can be substituted preferentially into the large framework-cation sites in ganomalite-type and nasonite-type structures, as well as in the structures of apatite polysomes of higher order. Such substitutions could conceivably be used to "fine-tune" the functionalities of such phases.

Acknowledgements

Reviewers xxx and yyy are thanked for their constructive comments on the manuscript. The microprobe analyses and some of the SEM work were funded by a grant to Caltech from the Northern California Mineralogical Society. The Caltech spectroscopic work was funded by NSF grant EAR-0947956. The remainder of this study was funded by the John Jago Trelawney Endowment to the Mineral Sciences Department of the Natural History Museum of Los Angeles County.

References

Baikie, T., Pramana, S.S., Ferraris, C., Huang, Y., Kendrick, E., Knight, K.S., Ahmad, Z., and White, T.J. (2010) Apatite polysomes. Acta Crystallographica, B66, 1–16.

Brese, N.E., and O'Keeffe, M. (1991) Bond-valence parameters for solids. Acta Crystallographica, B47, 192–197.

Brown, I.D., and Altermatt, D. (1985) Bond-valence parameters from a systematic analysis of the inorganic crystal structure database. Acta Crystallographica, B41, 244–247.

Burla, M. C., Caliandro, R., Camalli, M., Carrozzini, B., Cascarano, G.L., Giacovazzo, C., Mallamo, M., Mazzone, A., Polidori, G., and Spagna, R. (2012) SIR2011: a new package for crystal structure determination and refinement. Journal of Applied Crystallography, 45, 357–361.

Burnham, C.W. (1959), Contact metamorphism of magnesian limestones at Crestmore, California. Bulletin of the Geological Society of America, 70, 879–920.

Carlson, S., and Norrestam, R. (1997) The crystal structure of ganomalite, $Pb_9Ca_{5.44}Mn_{0.56}Si_9O_{33}$. Zeitschrift für Kristallographie, 212, 208–212.

DeVito, F., Parcel, R.T., and Jefferson, G.T. (1971). Contact metamorphic minerals at Crestmore quarry, Riverside, California: in Elders, WA ed., Geological excursions in southern California: Riverside, California, University California. Campus Museum Contribution, 1, 94–125.

Dunn, P.J., Peacor, D.R., Valley, J.W., and Randall, C.A. (1985) Ganomalite from Franklin, New Jersey, and Jakobsberg, Sweden: new chemical and crystallographic data. Mineralogical Magazine, 49, 579–592.

342 Engel, G. (1972) Ganomalite, an intermediate between the nasonite and apatite types.
343 Naturwissenschaften, 59, 121–122.
344 Forrester, C. (2004) Large clintonite crystals from the Crestmore Quarry, Riverside, California.
345 Mineralogical Record, 35, 325–330.
346 Hale, G.M., and Querry M.R. (1973) Optical constants of water in the 200-nm to 200-μm
347 wavelength region. Applied Optics, 12, 555–563.
348 Higashi, T. (2001) ABSCOR. Rigaku Corporation, Tokyo.
349 Hughes, J.M., and Rakovan, J. (2015) Structure, chemistry, and properties of apatite and apatite
350 supergroup minerals. *Elements*, 11, 165–170.
351 Krivovichev, S.V., and Brown, I.D. (2001) Are the compressive effects of encapsulation an
352 artefact of the bond valence parameters? Zeitschrift für Kristallographie, 216, 245–247.
353 Krivovichev, S.V. (2012) Derivation of bond-valence parameters for some cation-oxygen pairs
354 on the basis of empirical relationships between r_o and b. Zeitschrift für Kristallographie, 227,
355 575–579.
356 Lafuente, B., Downs, R.T., Yang, H., and Stone, N. (2015) The power of databases: the RRUFF
357 project. In: Highlights in Mineralogical Crystallography, T. Armbruster and R.M. Danisi,
358 eds., Berlin, Germany, W. De Gruyter, pp 1–30.
359 Mandarino, J.A. (2007) The Gladstone–Dale compatibility of minerals and its use in selecting
360 mineral species for further study. Canadian Mineralogist, 45, 1307–1324.
361 Nordenskiöld , A.E. (1876) Ganomalit. Geologiska Föreningen i Stockholm Förhandlingar, 3,
362 121.
363 Nordenskiöld, A.E. (1877) Nya mineralier från Långban. Geologiska Föreningen i Stockholm
364 Förhandlingar, 3, 382–384.

Pan, Y., and Fleet, M.E. (2002) Compositions of the apatite-group minerals: substitution mechanisms and controlling factors. In: Phosphates – geochemical, geobiological, and materials importance, M.J. Kohn, J. Rakovan, and J.M. Hughes, eds. Reviews in Mineralogy and Geochemistry, 48, 14–49.

Penfield, S.L., and Warren, C.H. (1899) Some New Minerals from the Zinc Mines at Franklin, NJ, and Note Concerning the Chemical Composition of Ganomalite**.** American Journal of Science, 8, 339–353.

Sheldrick, G.M. (2008) A short history of SHELX. Acta Crystallographica, A64, 112–122.

White, T., Ferraris, C., Kim, J., and Madhavi, S. (2005) Apatite – an adaptive framework structure. In: Micro- and mesoporous mineral phases, G. Ferraris and S. Merlino, eds. Reviews in Mineralogy and Geochemistry, 57, 307–401.

Wieliczka, D.M., Weng, S., and Querry, M.R. (1989) Wedge shaped cell for highly absorbent liquids: infrared optical constants of water. Applied Optics, 28, 1714–1719.

FIGURE CAPTIONS

Figure 1. Wayneburnhamite and whelanite (blades) on vesuvianite/wollastonite rock (holotype specimen); FOV 1.13 mm across.

Figure 2. Backscatter SEM image of wayneburnhamite on calcite (cotype specimen).

Figure 3. Crystal drawing of wayneburnhamite, clinographic projection.

Figure 4. Raman spectrum of wayneburnhamite from Crestmore compared to that of ganomalite from the Jacobsberg mine.

Figure 5. Infrared spectrum of wayneburnhamite from Crestmore.

Figure 6. Crystal structure of wayneburnhamite viewed along **c**. The positions of the electron density residuals corresponding to the Pb^{2+} $6s^2$ lone electron pairs are shown for one Pb tunnel. Note that the Ca2 and Ca4 polyhedra only appear to be twisted; it is the Ca1 and Ca3 polyhedra beneath them that are twisted.

Figure 7. Crystal structure of wayneburnhamite viewed along [110].

400 Table 1. Electron microprobe data (wt%) for wayneburnhamite.

Constituent	Mean	Range	St. dev.	Standard
PbO	66.08	65.06–66.93	0.72	galena
SrO	0.15	0.10–0.23	0.04	celestine
CaO	10.75	10.65–10.92	0.14	syn. anorthite
MnO	0.01	0.00–0.04	0.02	Mn olivine
CuO	0.76	0.35–1.47	0.43	cuprite
SiO_2	19.21	18.96–19.39	0.20	syn. anorthite
SO_3	0.59	0.37–0.80	0.20	galena
Cl	0.06	0.02–0.11	0.03	vanadinite
O=Cl	-0.01			
Total	97.60			

401
402
403

404 Table 2. Powder X-ray diffraction data (d in Å) for wayneburnhamite.
405

I_{obs}	d_{obs}	d_{calc}	I_{calc}	$h\ k\ l$
3	10.07	10.2054	2	0 0 1
17	8.57	8.5696	10	1 0 0
		6.5627	3	1 0 1
52	4.95	4.9477	62	1 1 0
64	4.45	4.4520	59	1 1 1
33	4.28	4.2848	32	2 0 0
8	3.93	3.9507	5	2 0 1
77	3.550	3.5521	84	1 1 2
39	3.403	3.4018	69	0 0 3
		3.2814	3	2 0 2
54	3.232	3.2390	52	1 2 0
		3.1618	19	1 0 3
100	3.086	3.0872	100	1 2 1
60	2.847	2.8565	66	3 0 0
48	2.798	2.8031	76	1 1 3
83	2.734	2.7346	88	2 1 2
		2.6642	2	2 0 3
4	2.468	2.4738	5	2 2 0
17	2.368	2.3768	16	3 1 0
18	2.337	2.3458	22	2 1 3
		2.3148	4	3 1 1
6	2.264	2.2676	13	1 1 4
		2.2260	3	2 2 2
7	2.189	2.1876	10	3 0 3
		2.1545	5	3 1 2
29	2.141	2.1424	29	4 0 0
42	1.9965	2.0042	22	2 1 4
		2.0007	27	2 2 3
27	1.9546	1.9660	18	3 2 0
		1.9483	31	1 3 3
35	1.9318	1.9305	28	3 2 1
20	1.8784	1.8868	24	1 1 5
		1.8700	6	1 4 0
25	1.8330	1.8345	31	3 2 2
46	1.8111	1.8128	51	4 0 3
		1.7558	2	1 4 2
		1.7391	4	1 3 4
24	1.7247	1.7268	29	2 1 5
15	1.7006	1.7022	9	3 2 3
		1.7009	14	0 0 6
		1.6407	2	4 0 4
		1.6281	4	3 3 1
13	1.6194	1.6195	8	4 2 0
		1.6085	3	1 1 6
		1.5995	3	2 4 1
		1.5809	3	2 0 6
8	1.5650	1.5693	5	3 3 2
		1.5573	7	2 3 4
		1.5485	2	3 1 5
12	1.5392	1.5436	4	2 4 2
		1.5391	12	1 5 0
		1.5306	2	5 0 3
15	1.5188	1.5219	15	1 5 1
4	1.4972	1.5059	8	2 1 6
		1.4840	2	3 3 3
		1.4736	19	5 1 2
25	1.4667	1.4622	6	2 4 3
		1.4614	11	3 0 6
		1.4160	17	3 2 5
17	1.4093	1.4088	6	4 3 0
		1.4023	11	1 5 3
		1.3832	3	1 3 6
		1.3673	2	2 4 4
		1.3600	4	2 5 1
		1.3321	9	4 0 6
		1.3294	3	1 2 7
11	1.3234	1.3252	5	2 5 2
		1.3179	5	1 5 4
		1.3169	3	6 0 3
12	1.2993	1.3016	16	4 3 3

406
407
408

Table 3. Data collection and structure refinement details for wayneburnhamite.

Diffractometer	Rigaku R-Axis Rapid II
X-ray radiation / power	MoK_α (λ = 0.71075 Å)/50 kV, 40 mA
Temperature	293(2) K
Structural Formula	$(Pb_{8.34}\square_{0.66})_{\Sigma 9.00}(Ca_{5.31}Cu^{2+}_{0.69})_{\Sigma 6.00}(Si_2O_7)_3(SiO_4)_3$
Space group	*P*–6
Unit cell dimensions	a = 9.8953(9) Å
	c = 10.2054(7) Å
V	865.41(17) Å^3
Z	1
Density (for above formula)	5.306 g cm^{-3}
Absorption coefficient	42.030 mm^{-1}
F(000)	1200.1
Crystal size	130 × 120 × 30 μm
θ range	3.10 to 24.98°
Index ranges	$-11 \le h \le 11$, $-11 \le k \le 11$, $-12 \le l \le 12$
Refls collected / unique	10512 / 1078; R_{int} = 0.073
Reflections with $F_o > 4\sigma(F)$	1063
Completeness to θ = 24.98°	99.3%
Refinement method	Full-matrix least-squares on F^2
Parameters / restraints	100 / 0
GoF	1.080
Final R indices [$F_o > 4\sigma(F)$]	R_1 = 0.0301, wR_2 = 0.0685
R indices (all data)	R_1 = 0.0303, wR_2 = 0.0686
Flack parameter	0.36(3)
Largest diff. peak / hole	+2.46 / –0.88 e/A^3

*$R_{int} = \Sigma|F_o^2\text{-}F_o^2(\text{mean})|/\Sigma[F_o^2]$. GoF = $S = \{\Sigma[w(F_o^2-F_c^2)^2]/(n-p)\}^{1/2}$. $R_1 = \Sigma||F_o|\text{-}|F_c||/\Sigma|F_o|$. $wR_2 = \{\Sigma[w(F_o^2-F_c^2)^2]/\Sigma[w(F_o^2)^2]\}^{1/2}$; $w = 1/[\sigma^2(F_o^2) + (aP)^2 + bP]$ where a is 0.0197, b is 17.28 and P is $[2F_c^2 + \text{Max}(F_o^2,0)]/3$.

Table 4. Atom coordinates and displacement parameters ($Å^2$) for wayneburnhamite.

	x/*a*	*y*/*b*	*z*/*c*	U_{eq}
Pb1*	0.26469(13)	0.26712(12)	0.17969(8)	0.0248(3)
Pb2*	0.98756(15)	0.25550(15)	1/2	0.0219(3)
Ca1*	1/3	2/3	0.3400(7)	0.0152(15)
Ca2	1/3	2/3	0	0.015(2)
Ca3	2/3	1/3	0.3249(7)	0.0115(15)
Ca4*	2/3	1/3	0	0.020(2)
Si1	0.4096(9)	0.3838(9)	1/2	0.0120(17)
Si2	0.0239(8)	0.4092(8)	0.1502(7)	0.0235(15)
O1	0.507(3)	0.152(2)	0.1584(16)	0.037(5)
O2	0.074(3)	0.374(3)	0	0.027(5)
O3	0.134(2)	0.5994(19)	0.1667(15)	0.026(4)
O4	0.157(3)	0.649(4)	1/2	0.030(6)
O5	0.350(2)	0.265(2)	0.3761(14)	0.023(4)
O6	0.0744(19)	0.319(2)	0.2541(16)	0.032(4)
O7	0.602(3)	0.469(3)	1/2	0.028(6)

	U^{11}	U^{22}	U^{33}	U^{23}	U^{13}	U^{12}
Pb1	0.0384(6)	0.0306(6)	0.0160(4)	-0.0057(3)	-0.0074(4)	0.0252(5)
Pb2	0.0167(7)	0.0200(7)	0.0290(7)	0.000	0.000	0.0093(6)
Ca1	0.018(2)	0.018(2)	0.010(3)	0.000	0.000	0.0088(10)
Ca2	0.019(3)	0.019(3)	0.008(5)	0.000	0.000	0.0093(17)
Ca3	0.010(2)	0.010(2)	0.015(4)	0.000	0.000	0.0050(11)
Ca4	0.020(3)	0.020(3)	0.018(5)	0.000	0.000	0.0101(16)
Si1	0.011(4)	0.008(4)	0.016(4)	0.000	0.000	0.004(3)
Si2	0.017(3)	0.029(4)	0.020(3)	0.002(3)	0.000(3)	0.008(3)
O1	0.039(10)	0.019(9)	0.038(11)	-0.012(8)	-0.027(9)	0.003(8)
O2	0.025(13)	0.031(13)	0.028(14)	0.000	0.000	0.017(11)
O3	0.024(10)	0.012(9)	0.034(11)	-0.010(6)	-0.009(7)	0.003(7)
O4	0.033(15)	0.045(18)	0.024(14)	0.000	0.000	0.028(15)
O5	0.041(10)	0.027(9)	0.017(8)	-0.006(7)	-0.005(7)	0.027(8)
O6	0.023(8)	0.046(10)	0.035(9)	0.021(8)	0.006(7)	0.023(8)
O7	0.036(16)	0.019(14)	0.026(13)	0.000	0.000	0.012(13)

*Refined site occupancies: Pb1 0.926(13), Pb2 0.928(14), Ca1/Cu1 0.80/0.20(6), Ca4/Cu4 0.71/0.29(8).

Table 5. Selected bond distances (Å) for wayneburnhamite.

Pb1–O5	2.180(15)	Ca1–O4(×3)	2.330(19)	Si1–O4	1.60(3)
Pb1–O3	2.292(19)	Ca1–O3(×3)	2.483(16)	Si1–O5(×2)	1.621(16)
Pb1–O6	2.316(16)	<Ca1–O>	2.407	Si1–O7	1.65(3)
Pb1–O1	3.14(3)			<Si1–O>	1.623
Pb1–O2	3.171(19)	Ca2–O3(×6)	2.435(18)		
Pb1–O1	3.28(3)	Ca2–O2(×3)	2.75(2)	Si2–O1	1.54(2)
Pb1–O6	3.372(18)	<Ca2–O>	2.540	Si2–O6	1.616(16)
<Pb1–O>	2.822			Si2–O3	1.646(18)
		Ca3–O1(×3)	2.403(17)	Si2–O2	1.698(13)
Pb2–O7	2.26(2)	Ca3–O7(×3)	2.50(2)	<Si2–O>	1.625
Pb2–O5(×2)	2.546(16)	Ca3–O5(×3)	2.901(16)		
Pb2–O6(×2)	2.625(16)	<Ca3–O>	2.601		
Pb2–O4(×2)	3.19(3)				
<Pb2–O>	2.740	Ca4–O1(×6)	2.35(2)		

Table 6. Bond valence sums for wayneburnhamite. Values are expressed in valence units.

	O1	O2	O3	O4	O5	O6	O7	Σ
Pb1	0.09 0.07	0.08 ×2↓	0.51		0.64	0.49 0.06		1.93
Pb2				0.08 0.05	0.30 ×2→	0.26 ×2→	0.55	1.80
Ca1			0.25 ×3→	0.37 ×2↓×3→				1.86
Ca2		0.12 ×3→	0.28 ×6→					2.04
Ca3	0.31 ×3→				0.08 ×3→		0.24 ×2↓×3→	1.89
Ca4	0.36 ×6→							2.16
Si1				1.07	1.01		0.93	4.01
Si2	1.25	0.82 ×2↓	0.94			1.02		4.03
Σ	2.08	1.92	1.98	1.94	2.03	1.83	1.96	

Multiplicity is indicated by ×↓→. All bond strengths are based upon full site occupancies by their dominant constituents. Pb^{2+}–O bond valence parameters are from Krivovichev and Brown (2001), Ca^{2+}–O from Brown and Altermatt (1985) and Si^{4+}–O from Brese and O'Keeffe (1991).

Figure 1

Figure 2

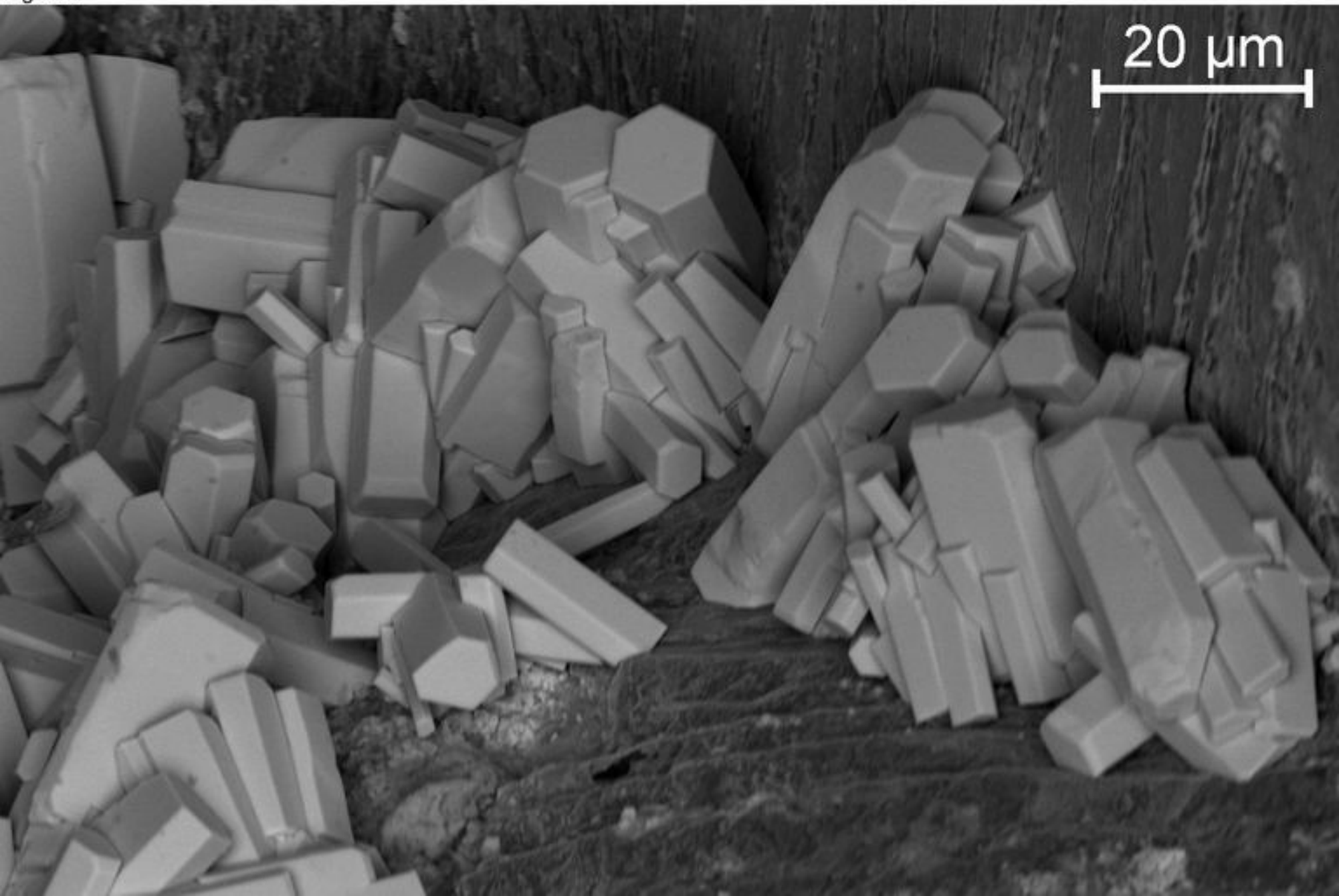

Figure 3

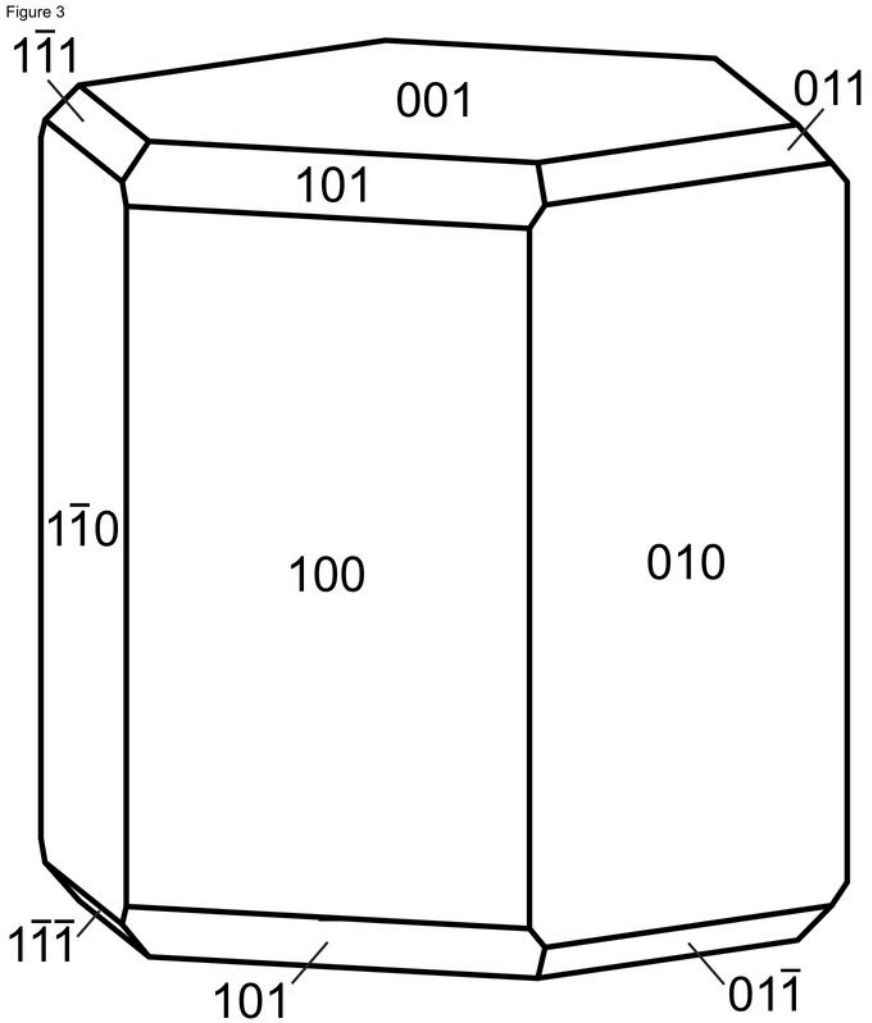

Figure 4

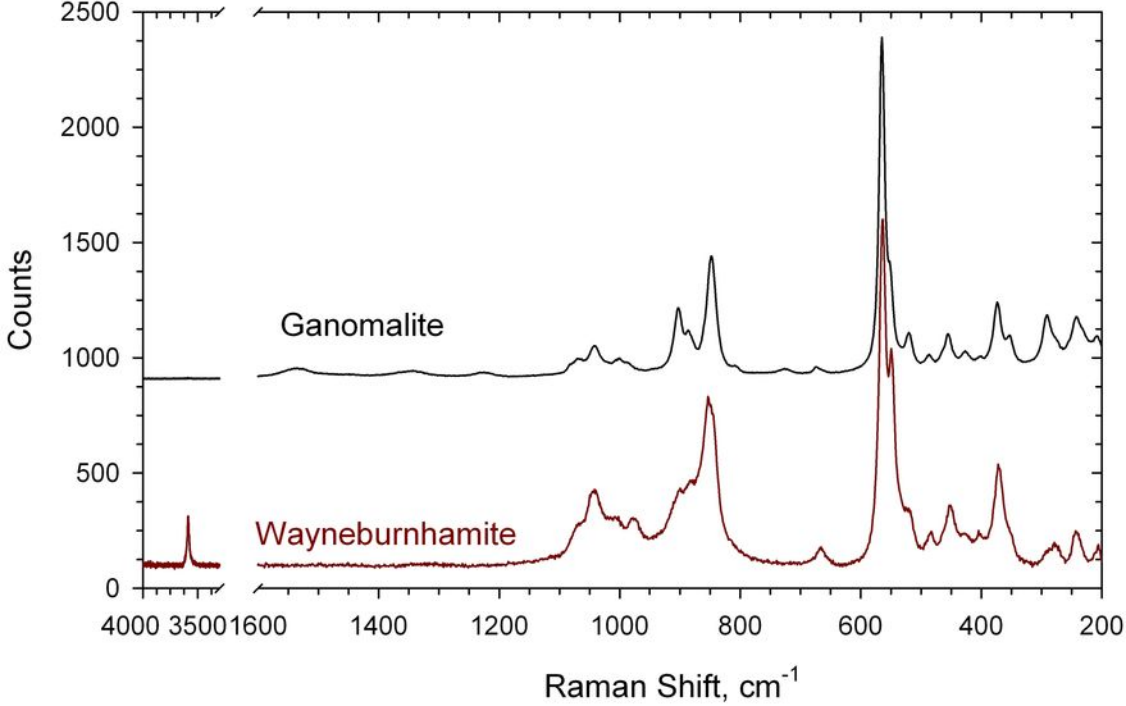
2500
2000
1500
1000
500
0
Counts
Ganomalite
Wayneburnhamite
4000
3500
1600
1400
1200
1000
800
600
400
200
Raman Shift, cm-1

Figure 5

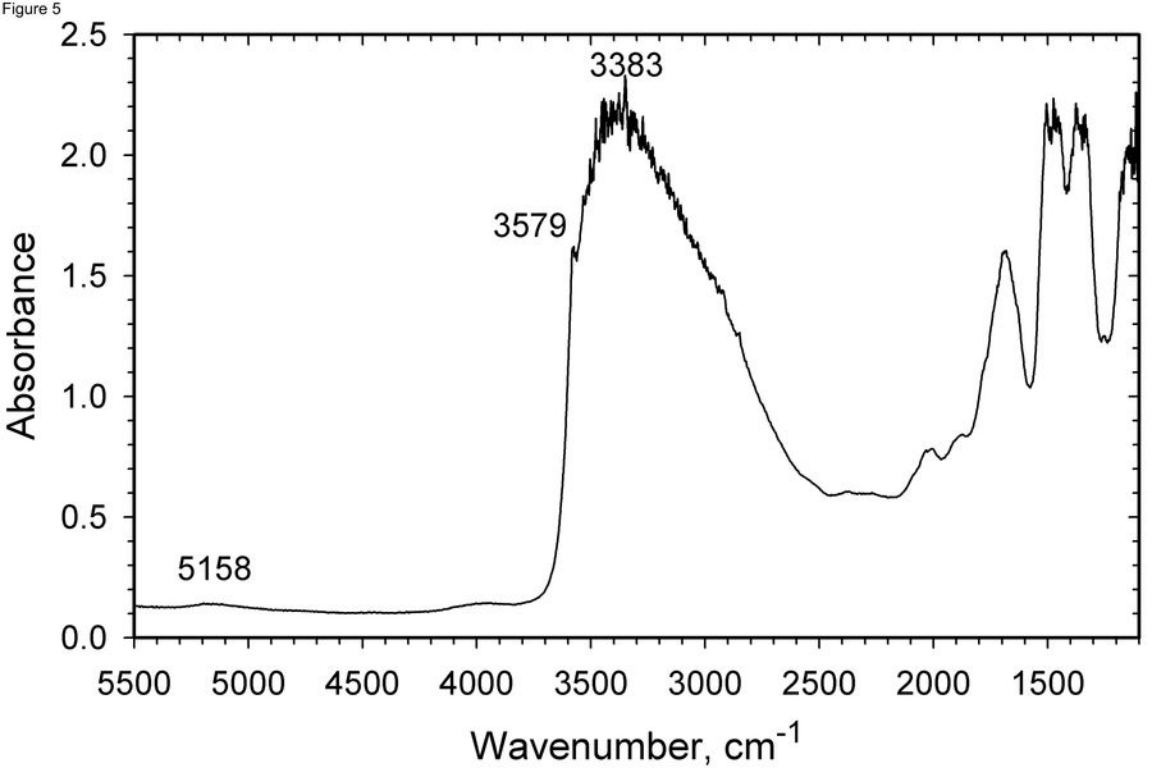
3383
3579
5158
Absorbance
Wavenumber, cm-1
2.5
2.0
1.5
1.0
0.5
0.0
5500
5000
4500
4000
3500
3000
2500
2000
1500

Figure 6

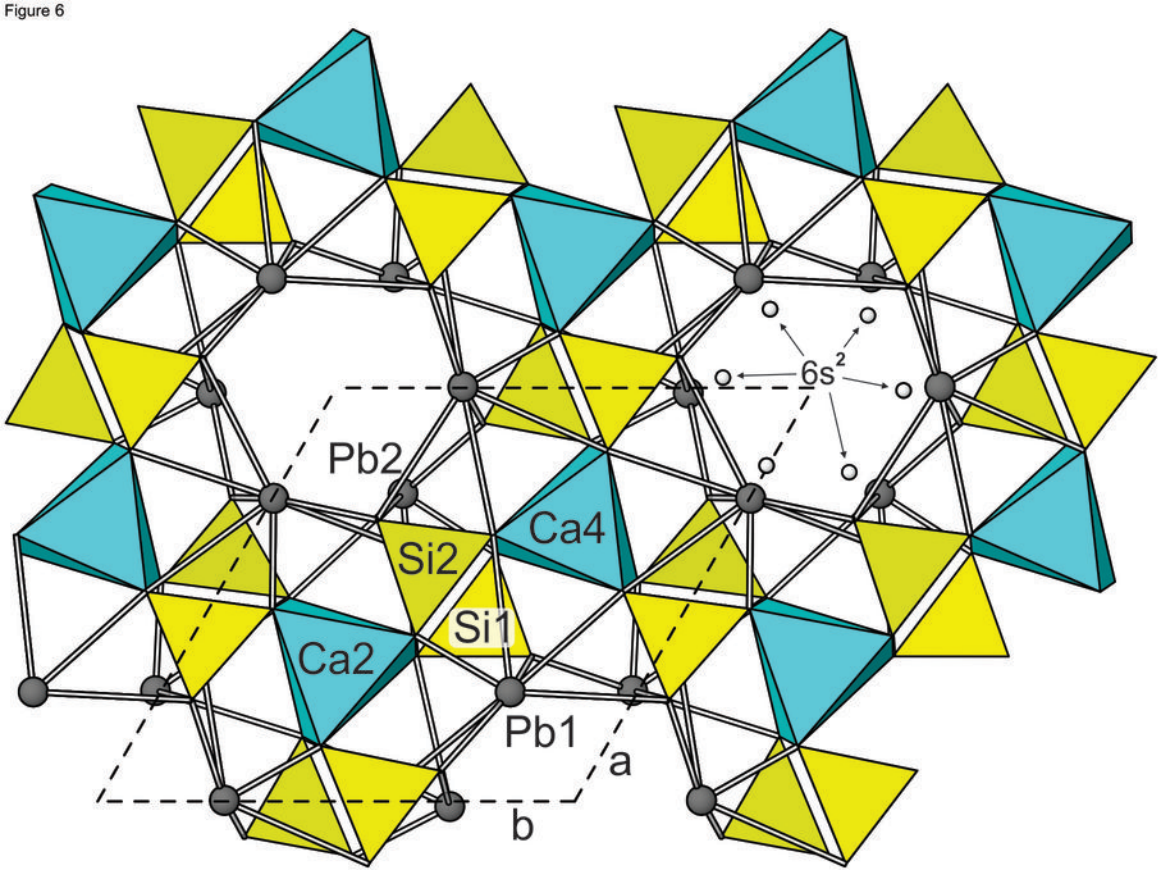

Figure 7